[9] K. Kurokawa, "Some basic characteristics of broadband negative resistance oscillator circuits," *Bell Syst. Tech. J.*, vol. 48, pp. 1937–1955, July/Aug. 1969.
[10] K. P. Weller, R. S. Ying, and D. K. Lee, "Pumps and local oscillators," Technical Report AFAL-TR-75-177 Air Force Avionics Laboratory, Sept. 1975.
[11] H. C. Okean and L. J. Steffek, "94 GHz parametric amplifier," Technical Report AFAL-TR-74-246 Air Force Avionics Laboratory, Dec. 1974.
[12] D. S. Peck, "Reliability predictions from accelerated testing," *9th Annual Proc. Reliability Physics Symposium*, Las Vegas, 1971.
[13] T. E. Seidel and D. L. Scharfetter, "High-power millimeter wave IMPATT oscillators with both hole and electron drift spaces made by ion implantation," *Proc. IEEE*, vol. 58, pp. 1135–1136, July 1970.
[14] K. P. Weller, A. B. Dreeben, H. L. Davis, and W. M. Anderson, "Fabrication and performance of GaAs p+n, junction and Schottky barrier millimeter IMPATT's," *IEEE Trans. Electron Devices*, vol. ED-21, pp. 25–31, Jan. 1974.
[15] K. Nawata, M. Ikeda, and Y. Ishii, "Millimeter-wave GaAs Schottky-barrier IMPATT diodes," *IEEE Trans. Electron Devices*, vol. ED-21, pp. 128–130, Jan. 1974.
[16] G. A. Swartz, Y. Chiang, C. P. Wen, and A. Gonzalez, "Performance of P-type epitaxial silicon millimeter-wave IMPATT diodes," *IEEE Trans. Electron Devices*, vol. ED-21, pp. 165–171, Feb. 1974.
[17] R. E. Goldwasser and J. F. Caldwell, "Millimeter wave Gunn devices," presented at WESCON, Los Angeles, Sept. 1974.
[18] P. Staecker, "*Ka*-band IMPATT diode reliability," presented at the International Conf. Electron Devices, Washington, DC, Dec. 1973.
[19] N. B. Kramer, "Millimeter IMPATT diode progress," presented at IEEE INTERCON, New York, March 1974.
[20] N. B. Kramer, "Millimeter IMPATT devices," presented at WESCON, Los Angeles, Sept. 1974.
[21] D. S. Matthews, private communication.
[22] R. Bosch and H. W. Thim, "Computer simulation of transferred electron devices using the displaced Maxwellian approach," *IEEE Trans. Electron Devices*, vol. ED-21, pp. 16–25, Jan. 1974.
[23] E. J. Denlinger, J. Rosen, E. Mykietyn, and E. C. McDermott, Jr., "Microstrip varactor-tuned millimeter-wave IMPATT diode oscillators," *IEEE Trans. Microwave Theory Tech.*, vol. MTT-23, pp. 953–958, Dec. 1975.
[24] M. Gilden and M. E. Hines, "Electronic tuning effects in the Read microwave avalanche diode," *IEEE Trans. Electron Devices*, vol. ED-13, pp. 169–175, Jan. 1966.
[25] C. Chao, unpublished work.
[26] M. Ohtomo, "Experimental evaluation of noise parameters in Gunn and avalanche oscillators," *IEEE Trans. Microwave Theory Tech.*, vol. MTT-20, pp. 425–437, July 1972.
[27] K. P. Weller, unpublished work.
[28] H. Okamoto, "Noise characteristics of GaAs and Si IMPATT diodes for 50-GHz range operation," *IEEE Trans. Electron Devices*, vol. ED-22, pp. 558–565, Aug. 1975.
[29] W. V. T. Rusch and C. A. Burrus, "Planar millimeter-wave epitaxial silicon Schottky-barrier converter diodes," *Solid State, Electronics*, vol. 11, pp. 517–525, 1968.
[30] H. M. Leedy, H. L. Stover, H. G. Morehead, R. P. Bryan, and H. L. Garvin, "Advanced millimeter-wave mixer diodes, GaAs and silicon, and a broadband low-noise mixer," presented at the Conf. High Frequency Generation and Amplification, Cornell Univ., Ithaca, NY, August 1971.
[31] G. T. Wrixon, "Low-noise diodes and mixers for the 1–2 mm wavelength region," *IEEE Trans. Microwave Theory Tech.*, vol. MTT-22, pp. 1159–1165, Dec. 1974.
[32] D. T. Young and J. C. Irvin, "Millimeter frequency conversion using N-type GaAs Schottky-barrier epitaxial diodes with a novel contacting technique," *Proc. IEEE*, vol. 53, pp. 2130–2131, Dec. 1965.
[33] Y. Chang, H. J. Kuno, and D. L. English, "High data-rate millimeter-wave transmitter module," *IEEE Trans. Microwave Theory Tech.*, vol. MTT-23, pp. 470–477, June 1975.
[34] C. B. Swan, "Improved performance of silicon avalanche oscillators mounted on diamond heat sinks," *Proc. IEEE*, vol. 55, pp. 1617–1618, Sept. 1967.
[35] R. S. Ying and D. L. English, unpublished work.
[36] This procedure was developed by H. H. Luckey.
[37] D. Rubin, "Wide-bandwidth millimeter-wave Gunn amplifier in reduced-height waveguide," *IEEE Trans. Microwave Theory Tech.*, vol. MTT-23, pp. 833–834, Oct. 1975.

Highly Reliable High-Power 86-GHz Components and Transmitter–Receiver Modules

MASAMI AKAIKE, MEMBER, IEEE, HARUHIKO KATO, AND NOBORU KANMURI, MEMBER, IEEE

Abstract—**The reliability of semiconductor active devices is related to the junction temperature of diodes used. This paper describes the reliability design and performance of 86-GHz active components and transmitter–receiver modules for a guided millimeter-wave transmission system. The components are IMPATT oscillators, IMPATT amplifiers, varactor frequency multipliers, and Schottky-barrier diode upconverters. The maximum output powers of these active devices are calculated for a given mean time between failure (MTBF). Active components and transmitter–receiver modules for 86-GHz operation were manufactured based upon the design with considerations for reliability as well as RF performance.**

Manuscript received February 3, 1976; revised May 5, 1976.
The authors are with the Yokosuka Electrical Communication Laboratory, Nippon Telegraph and Telephone Public Corporation, Yokosuka-shi, Kanagawa-ken, Japan.

I. INTRODUCTION

IN RECENT YEARS guided millimeter-wave transmission systems have been intensively investigated in various countries in the world for the purpose of meeting growing demands in communications in the near future. There have been publications concerned with the system design, repeaters, and overall transmission tests [1]–[7].

There are basically two means of getting the millimeter-wave modulated carrier power; an upconverter [3], [4], [6], [7] and a millimeter-wave modulator [2], [3], [5], both of which have their own merits with respect to the circuit construction, output power and system design. The guided millimeter-wave transmission system in Japan,

W-40G, uses the frequency range 43–87 GHz and offers 300 000 telephone channels in both directions through a single circular waveguide line by means of 806-Mb/s 4-phase-PSK format [7]. The repeater employs an upconverter and, if necessary, the output power of the upconverter is amplified by a negative-resistance IMPATT amplifier. A description of the system is presented in detail in [7]. A repeater consists of five panels, the transmitter–receiver panel, modulator–demodulator panel, delay-equalizer panel, alarm-control panel, and power-supply panel. The transmitter–receiver panel is the high-frequency portion of the repeater and has a function of converting the millimeter-wave signals to IF signals and vice versa.

In order to realize a highly reliable high-power low-noise system, one must consider the junction temperature of diodes, which is a measure of diode reliability. The main problem in realizing such a system is how one allots the reliability to each component of the system. In papers which have so far been published concerned with active solid-state devices for guided millimeter-wave transmission systems, quantitative discussion of the reliability of devices or systems in that sense have not been made. Recently, considerable research has been performed on millimeter-wave diodes, such as Schottky-barrier diodes, p-n-junction varactor diodes, and IMPATT diodes, with respect to the relation between their junction temperatures and reliability [8]–[10].

The purpose of this paper is to show the optimum design and actual performance of 86-GHz high-power active solid-state devices and 86-GHz transmitter–receiver panels. They are designed so as to give the maximum output power under a given reliability condition. The construction of the transmitter–receiver panel is discussed; the main active devices are identified which are considered further in the succeeding discussion; and the reliability relationships of the millimeter-wave diodes are summarized. Optimum power design of the local oscillator (LO) and the transmitter portion of the panel is then described. This includes a comparison of two cases, one where the transmitter–receiver panel has only an upconverter and another where the upconverter is followed by a negative-resistance IMPATT amplifier. The actual performances of upconverters, LO's, IMPATT amplifiers, and overall system characteristics of the 86-GHz transmitter–receiver panels are also presented.

II. Component Design Descriptions

A. Construction of Transmitter–Receiver Panel

Fig. 1 shows the block diagram of a transmitter–receiver panel. Conversion of millimeter-wave and IF signals is performed by an upconverter and a downconverter. Both the upconverter and downconverter are excited by a common LO. The single-ended mixer frequency converters employ n-type GaAs Schottky-barrier diodes. Following the upconverter, an IMPATT amplifier can be connected to amplify the upconverter output power. In this case the overall reliability should be kept unchanged compared with the panel without an amplifier. The LO consists of an

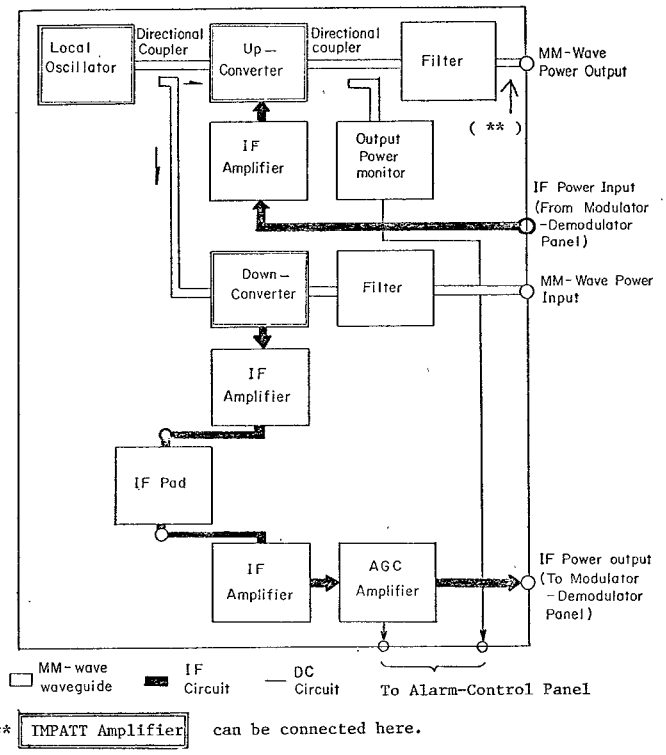

Fig. 1. Block diagram of the transmitter–receiver panel.

IMPATT source oscillator, a frequency multiplier, and an IMPATT amplifier. In the IMPATT source oscillator and amplifier Si single-drift-region-type IMPATT diodes are used. The frequency of the LO is stabilized by means of a cavity-loaded source oscillator. In the frequency multiplier a p^+-n-type GaAs diffused-junction varactor diode is used. Every diode is encased in a waveguide wafer-type diode holder. Both the waveguide windows and IF terminal of the waveguide wafer-type diode holder are hermetically sealed to protect the diode.

B. Reliability of Millimeter-Wave Diodes

The mean time between failure (MTBF) T of well-screened millimeter-wave diodes is determined by its junction temperature. Recently, research on the relation between MTBF and junction temperature has been performed by life-testing diodes at different temperatures [8]–[10]. According to the experimental results obtained by Sato and Suzuki, those relations are expressed by the following empirical formulas [9], [10]:[1]

$$T = 4.9620 \times 10^{-10} \times \exp\left[1.3429 \times 10^4/T_j\right]$$

(n-type GaAs Schottky-barrier diode) (1)

$$T = 3.0902 \times 10^{-10} \times \exp\left[1.6705 \times 10^4/T_j\right]$$

(Si single-drift-region-type IMPATT diode) (2)

[1] The life test was conducted with millimeter-wave diodes of different temperatures. Diodes were tested under two conditions. Half of the diodes were kept within ovens and the other half were applied with dc current. Both the temperature of the oven and dc current had more than three levels. According to the life test, failure occurred when the electrode metal got into the semiconductor junction.

$$T = 7.7202 \times 10^{-7} \times \exp\left[1.1815 \times 10^{4}/T_j\right] \quad (p^{+}n\text{-type GaAs varactor diode}) \quad (3)$$

where T_j is the junction temperature of the diode in degrees Kelvin and T is MTBF in hours.

C. IMPATT Amplifier

Ohmori investigated the oscillator power, junction temperature rise, and junction diameter of 80-GHz IMPATT diodes [11]. According to his results, when the junction diameter is optimized, the maximum oscillator power P_{osc} (milliwatts) can be expressed as a function of junction temperature rise ΔT_j (degrees Celsius) and constants which are determined by diode parameters, such as impurity concentration profile, conductivity and thickness of the semiconductor, and thermal resistance of the diode, as follows[2]:

$$P_{osc} = 7.686 \times 10^{-3} \times \Delta T_j^{1.786}. \quad (4)$$

The negative conductance of an IMPATT diode is a function of the RF voltage across the diode. The relation between the negative conductance $-G$ and RF voltage V_D is approximately expressed as [12]-[14]

$$G = G_M \cdot (V_M - V_D)^2/V_M^2 \quad (5)$$

where G_M is the maximum absolute value of the negative conductance, and V_M is the RF voltage across the diode when the negative conductance becomes zero. The load is connected through an impedance transformer. Here, let us neglect the loss of the impedance transformer and the series resistance of the IMPATT diode.

For an amplifier using a diode with the characteristic shown in (5), the output power of the amplifier changes depending upon input power level, and the relation among the ratio (μ) of the maximum output power of the amplifier to the maximum diode oscillation power, gain compression ξ, and power gain G_A may be given by

$$\mu = \frac{\sqrt{\xi G_A} + 1}{\sqrt{\xi G_A} - 1} \cdot \frac{4G_A}{(1 + \sqrt{G_A})^2} \cdot \left(1 + \frac{\sqrt{\xi G_A} + 1}{\sqrt{\xi G_A} - 1} \cdot \frac{1 - \sqrt{G_A}}{1 + \sqrt{G_A}}\right). \quad (6)$$

Derivation of (6) is shown in the Appendix. Fig. 2 is the schematic representation of (6). Dots show the experimental data. When the compression is low and the gain is high, the amplifier output power is below the oscillation power, but as the compression becomes higher or the gain becomes lower, the amplifier output power becomes comparable to the oscillation power and then exceeds it.

[2]Equation (4) was obtained by drawing the envelope of curves given by Ohmori's theoretical and experimental investigations [11, fig. 1]. Equation (4) would vary depending upon the impurity concentration profile, conductivity, and thickness of semiconductor used. However, since diodes described in this paper were fabricated in a similar manner to that described in [11], the authors adopt this equation for designing IMPATT devices.

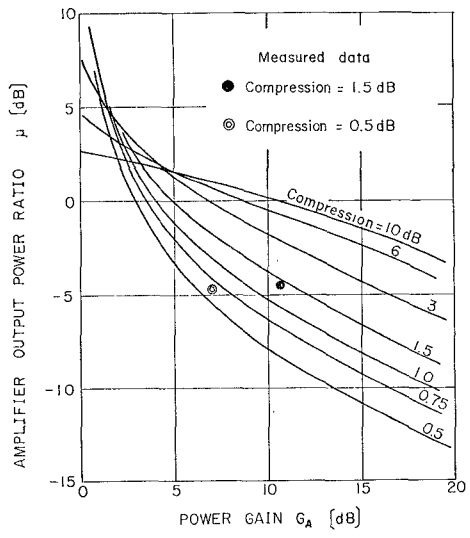

Fig. 2. Amplifier output ratio μ (= amplifier output power/oscillator output power) as a function of power gain of an IMPATT diode.

TABLE I
COMPRESSION AND CONVERSION LOSS OF AN UPCONVERTER

Compression [dB]	0.5	1.0	1.5	2.0
Conversion Loss [dB]	9.0	8.0	6.9	5.6
P_L [dBm] - P_{IF} [dBm]	4.0	2.2	1.0	0.1

D. Upconverter

The conversion loss of an upconverter is a function of LO and IF power levels and compression of the output power. When the IF power is sufficiently low compared with the LO power, the output power increases linearly with the IF power. However, when the IF power becomes comparable to the LO power, output compression occurs due to the saturation effect of the nonlinear conductance of the diode. The value of compression depends upon the difference between LO and IF powers. These relations have been examined experimentally with a GaAs Schottky-barrier diode with a diameter of 7 μm. The results are shown in Table I. They have approximately linear relations.

The junction temperature rise of the diode is determined by the thermal resistance of the diode and the power dissipation at the junction. The powers incident to the diode are the LO and IF powers. The junction temperature rise ΔT_j is given by the thermal resistance R_θ, the incident LO power P_L, and the incident IF power P_{IF} as

$$\Delta T_j = kR_\theta \cdot (P_L + P_{IF}) \quad (7)$$

where k is a factor determined by power dissipation distribution near the diode junction. The incident powers are converted to the output signal power, dc power, image, and other higher harmonics, which are absorbed by the external circuits. Moreover, since the series resistance of a diode is distributed around the junction, the power dissipated by the series resistance which is located far from the diode junction does not contribute to the junction temperature rise. According to the calculation for a 7-μm diode at 80 GHz, k was obtained as 0.33 [15]. The thermal resistance

is given by Torrey and Whitmer [16]. For a 7-μm n-type GaAs Schottky-barrier diode in which the whisker is made of gold, R_θ = 1620 °C/W.

E. Frequency Multiplier

For the junction temperature rise of the varactor diode in a frequency multiplier, discussion similar to that of the Schottky-barrier diode in an upconverter was made by Kato and Kaneko [17]. According to their results, for a varactor multiplier whose input frequency is in the microwave or millimeter-wave frequency range, power dissipation is distributed inside the skin layer of the semiconductor. In this case the thermal resistance reduces by a factor of 1/2–1/3 compared with the value calculated with the assumption that the power is dissipated just at the junction [17].

III. Subsystem Design Tradeoffs

A. Local Oscillator

Two versions of the LO are considered: 1) The millimeter-wave power is obtained by means of a cavity-locked source oscillator and a frequency multiplier, followed by an IMPATT amplifier. 2) A cavity-locked millimeter-wave IMPATT oscillator is followed by an IMPATT amplifier. Design parameters of the LO are 1) output power, 2) reliability, and 3) frequency stability and noise. In the present transmitter–receiver panel a high-Q cavity and a filter are used to satisfy the specifications on frequency stability and noise. Only the relation between the output power and reliability, and reliability allotment to each component of the LO, are described here.

Let us assume the following conditions in calculating the LO reliability.

1) The MTBF of a component, such as an amplifier, an upconverter or a frequency multiplier, is determined by the junction temperature of the diode used.

2) IMPATT diodes are of Si single-drift-region type and varactor diodes are of GaAs p^+-n-type.

3) The relation between junction temperature and reliability does not depend upon frequency.

4) The oscillation power of an IMPATT diode is given by (4) and its frequency dependence is $1/f^2$, that is, the junction temperature rise of the diode ΔT_j (degrees Celsius) is given by P_{osc} (milliwatts) and f [GHz] as

$$\Delta T_j = 15.27 \times P_{osc}^{0.56} \times [f/80]^{1.12}. \quad (8)$$

5) The amplifier output power P_{amp} decreases by a factor of μ with respect to the maximum oscillator output power P_{osc}: $P_{amp} = \mu P_{osc}$. The power gain G_A, output compression ξ, and μ are related by (6). To reduce the number of parameters in calculation, the compression is set at 3 dB.

Expected losses of circuit components at 80 GHz in the LO and thermal resistances of varactor diodes are shown in Table II.

From (2)–(8) and Table II one can calculate the LO output power with respect to its MTBF (or failure rate). Fig. 3(a) shows MTBF T (hours) and failure rate R (fits) of the LO as a function of its output power for various maximum oscillation powers P_{osc} in the case where the LO uses a tripler as the frequency multiplier. Each broken line shows T or R versus a given P_{osc}. Therefore the envelope of those curves shows the maximum output power as a function of MTBF (or of failure rate). One can calculate the curves for the cases where the frequency multiplier is a doubler and is a quadrupler (for construction [A]), and

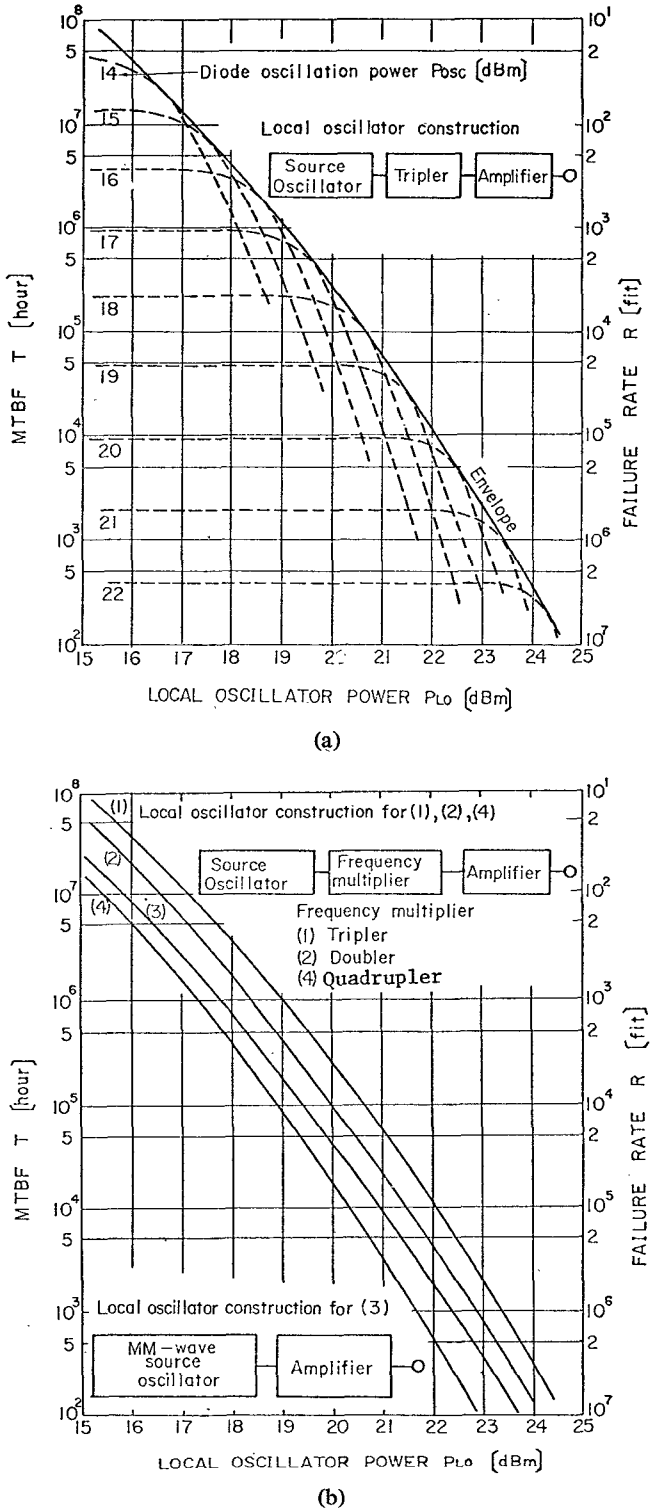

Fig. 3. Reliability versus output power of the LO. (a) Reliability of the LO for various P_{osc}. P_{osc} is the maximum oscillation power of the diode used in the amplifier. (b) Reliability versus maximum output power of the LO for constructions [A] and [B].

TABLE II
CIRCUIT LOSS AND THERMAL RESISTANCE OF LOCAL OSCILLATOR COMPONENTS

Loss, Thermal Resistance	[A]			[B]
	Doubler	Tripler	Quadrupler	
Cavity Loss [dB]	0.5	0.5	0.5	3.0
Conversion Loss [dB]	6.3	7.8	11.5	
Input circuit Loss of Multiplier [dB]	0.4	0.4	0.4	Output of Source Oscillator ~ Input of Amplifier = 0.5
Output Circuit Loss of Multiplier [dB]	1.1	1.1	1.1	
Thermal Resistance of Varactor [oC/W]*	350	350	280	

* Junction diameters are 20 μm for the doubler and the tripler and 27 μm for the quadrupler. Listed value is one-half the value calculated [16] from junction diameter. The reason is shown in the text.

TABLE III
RELIABILITY ALLOTMENT OF LOCAL OSCILLATORS

Local-Oscillator Construction		Local-Oscillator Output [dBm]	Junction Temperature Rise [°C]*			Failure Rate [fit]*			
			ΔT_{J1}	ΔT_{J2}	ΔT_{J3}	R_1	R_2	R_3	$R_1+R_2+R_3$
[A]	Doubler	20.0	192.7	80.1	190.8	5309	35	4656	10^4
	Tripler	20.6	179.5	144.4	190.8	2132	3252	4656	10^4
	Quadrupler	18.9	133.3	149.8	193.0	49	4505	5409	10^4
[B]		19.5	193.7		190.8	5678		4656	10^4

* Subscripts 1, 2, and 3 show source oscillator, multiplier, and amplifier, respectively.

for the case where the frequency multiplier is not used (for construction [B]). Fig. 3(b) is the relation between the maximum LO output power and reliability for constructions [A] and [B]. Table III shows the reliability allotment for the case where the total failure rate of the LO is 10^4 fits (MTBF = 10^5 h).

Fig. 3 and Table III indicate that 1) MTBF decreases by one order of magnitude with increase in LO power of 1.5 dB; 2) for the LO in which a frequency multiplier is used, a tripler or a doubler gives more power when compared with a quadrupler; 3) since at present a cavity loss of 3 dB is inevitable in the 80-GHz band, the LO in which a frequency multiplier is used gives more power; 4) the amplifier has about the same failure rate for all cases, and has about 50 percent of the total failure rate.

B. Transmitter Power with and without IMPATT Power Amplifier

The output power of the amplifier P_{amp} connected to an upconverter is expressed as

$$P_{amp} = P_L \cdot \eta \cdot G_A/L_1 \tag{9}$$

where P_L is the LO power incident to the upconverter and η is the conversion efficiency of the upconverter; L_1 is the connecting circuit loss from the output port of the upconverter to the input port of the amplifier; G_A is the amplifier power gain. The transmitter power P_{out} is

$$P_{out} = P_{amp}/L_2 \tag{10}$$

where L_2 is the circuit loss from the amplifier output port to the panel output port.

TABLE IV
CONNECTING CIRCUIT LOSS (DECIBELS)

Connecting Circuit		Panel with Amplifier	Panel without Amplifier
Local-Oscillator Output~Up-Converter Input		1.5	1.5
Up-Converter Output~IMPATT Amplifier Input	(l_1)*	2.5	
IMPATT Amplifier Output~Panel Output	(l_2)**	2.0	
Up-Converter Output~Panel Output	(l_3)***		3.0

Note: Connecting circuits are, * three circulators and one bandpass filter, ** two circulators and one directional coupler for monitoring power, and *** two circulators, one bandpass filter, one directional coupler, and one straight waveguide.

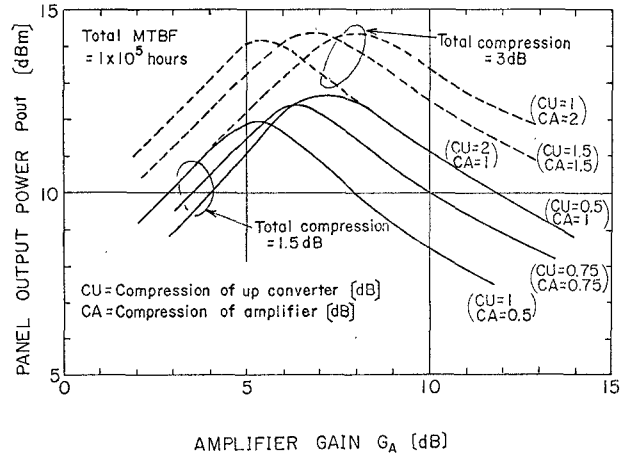

Fig. 4. Panel output power as a function of amplifier gain for various compressions. Total MTBF = 1 × 10^5 h.

In the panel without an amplifier P_{out} is given by

$$P_{out} = P_L \cdot \eta/L_3 \tag{11}$$

where L_3 is the connecting circuit loss from the upconverter output port to the panel output port.

From (1)–(11) one can calculate the transmitter power and reliability of the millimeter-wave portion of the transmitter–receiver panel. The millimeter-wave portion includes the LO upconverter and IMPATT amplifier. Since in the downconverter, power dissipation is sufficiently low compared with its power-handling capability, the contribution of the downconverter to increase in the total failure rate is negligible. Losses of connecting circuits L_1, L_2, and L_3 and the loss between the LO output port and upconverter input port are listed in Table IV.

Figs. 4–6 show the relation between the panel output power and reliability for two kinds of transmitter–receiver panels. One has only an upconverter (panel UP), and the other has an amplifier following the upconverter (panel AP). Data shown in Figs. 4–6(a) are results for panel AP, and Fig. 6(b) is for panel UP.

Fig. 4 shows the transmitter output power (panel output power) P_{out} as a function of amplifier gain when the total compression is 1.5 and 3 dB and the total MTBF (combined for the LO, upconverter, and amplifier) is 10^5 h. For the left arm of the curve, the output power is limited by MTBF's of the upconverter and LO, and for the right arm, it is restricted by the MTBF of the amplifier. The output power increases with compression. However, when the com-

TABLE V
RELIABILITY ALLOTMENT AND POWER LEVELS OF THE TRANSMITTER–RECEIVER PANEL

Total failure rate [fit]	Local oscillator		Up-converter			IMPATT amplifier				Panel output power [dBm]
	Output power [dBm]	Failure rate [fit]	Output power [dBm]	Junction temperature rise [°C]	Failure rate [fit]	Gain [dB]	Output power [dBm]	Junction temperature rise [°C]	Failure rate [fit]	
10^3	18.5	4.80×10^2	9.0	64.0	1.56×10^2	6.3	12.8	159.2	4.37×10^2	10.8
10^4	20.0	3.92×10^3	10.5	80.1	7.55×10^2	6.4	14.4	192.0	5.05×10^3	12.4
10^5	21.7	5.55×10^4	12.2	106.5	7.66×10^3	6.2	15.9	222.6	3.76×10^4	13.9

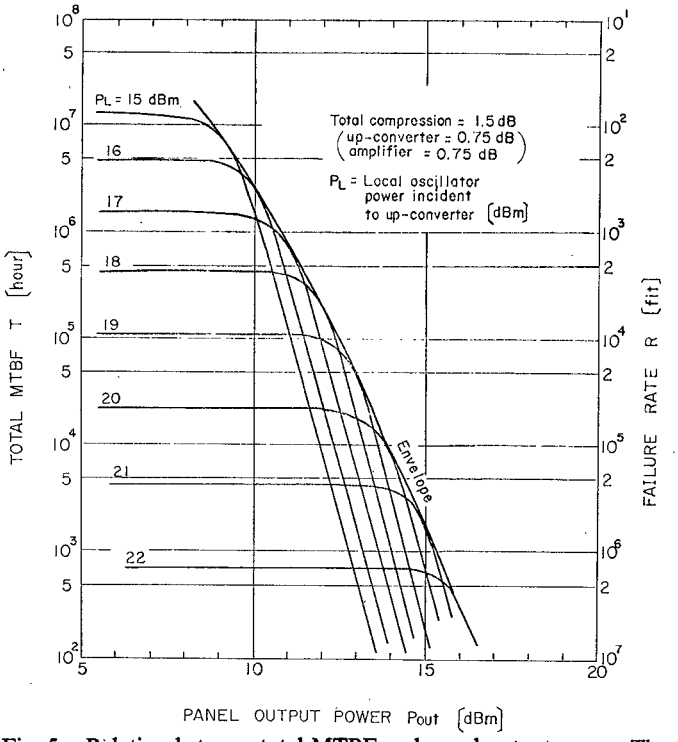

Fig. 5. Relation between total MTBF and panel output power. The envelope shows the relation when the gain is optimized. Total compression = 1.5 dB, and both the upconverter and amplifier have the same compression of 0.75 dB.

pression increases the degradation in pulsed waveform may occur. In the W-40G system the compression was determined to be less than 1.5 dB from the experimental data [7]. When the gain is 5–7 dB, the maximum output power is obtained. Fig. 5 shows the MTBF versus P_{out} for various values of the LO power P_L incident to the upconverter, where the total compression is 1.5 dB and both the upconverter and amplifier have the same compression of 0.75 dB. When P_{out} is low, the MTBF does not change with P_{out}. In this region the total MTBF is determined by the LO. When P_{out} increases, however, the MTBF of the amplifier becomes dominant and P_{out} decreases by about 1 dB with the increase in MTBF by one order of magnitude. The envelope of these curves shows the maximum output power when the gain is optimized. An output power of 12.5 dBm is expected for the case where the total MTBF is 10^5 h. Table V shows the power level of each component and reliability allotment when the total reliability is fixed. Fig. 6(a) shows the relation between the total MTBF and

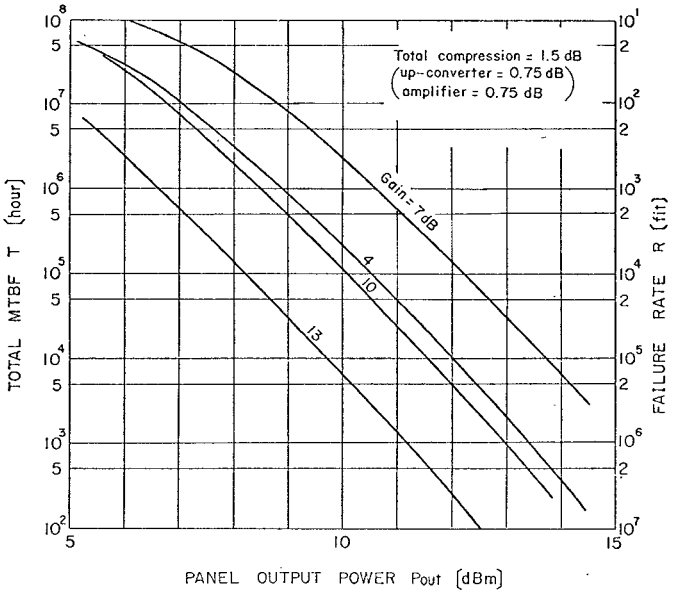

(a)

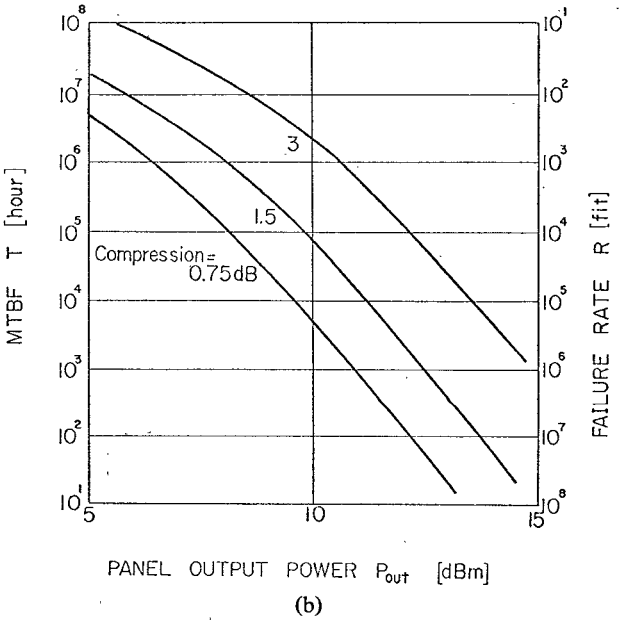

(b)

Fig. 6. Relation between the panel output power and reliability. (a) Reliability and panel output power for various amplifier gains. (b) Reliability and panel output power for various compressions of the upconverter. Panel AP: the panel with an IMPATT amplifier. Panel UP: the panel without an IMPATT amplifier.

the panel output power for various amplifier gains when the total compression is 1.5 dB and both the upconverter and amplifier have the same value 0.75 dB. When the gain is kept constant, the output power decreases by 1.5 dB with the increase in MTBF by a factor of 10. Fig. 6(b) shows MTBF versus P_{out} for various compressions of the upconverter. Fig. 6 tells us that the panel output power increases by 2.5 dB by introducing an IMPATT amplifier following the upconverter.

IV. Description of System Hardware

According to design considerations described in the preceding sections, two transmitter–receiver panels have been built. One employs an upconverter on the output stage (panel UP), and the other has an IMPATT amplifier following the upconverter (panel AP). Both of them were designed to have the same MTBF with respect to the millimeter-wave portion.

A. Local Oscillator

The LO described here consists of a source oscillator whose frequency is stabilized by means of a high-Q cavity, a tripler or a doubler, and an IMPATT amplifier. Since a tripler or a doubler gives more LO power when compared with either a quadrupler or the case without a frequency multiplier, these two multipliers were tested. The doubler was used in panel UP and the tripler was in panel AP. Oscillation frequencies of the source oscillators are 28.217 GHz for panel UP and 42.325 GHz for panel AP, respectively. The resonant mode of the cavity is the cylindrical TE_{012} mode, and the measured unloaded Q is about 9000 at 42 GHz.

The frequency multiplier has a crossed waveguide configuration and the diode is placed at the junction. The tripler is composed of three kinds of waveguides and a coaxial circuit which couples these waveguides. The waveguides are the R-260[3] for input, R-320[3] for idler termination, and R-740[3] for output. In this tripler, the conversion loss is 9 dB and the output power is 14 dBm when the input is 23 dBm. The doubler has two waveguides: R-500[3] for input and R-740[3] for output. The output is 11.5 dBm and the conversion loss is 7.3 dB. The estimated junction temperature rise is 63°C for the tripler diode and 55°C for the doubler. The frequency change is less than $\pm 7 \times 10^{-5}$ for the ambient temperature 0–50°C.

Fig. 7 shows block diagrams of the LO's in panel UP and panel AP. Power levels at various planes are shown in the figure: the source-oscillator output powers at point A are 23.0 dBm (panel UP) and 19.4 dBm (panel AP), and the LO output powers at point B are 18.7 dBm (panel UP) and 18.8 dBm (panel AP). As some part of the total failure rate should be alloted to the signal power amplifier in panel AP, the junction temperature of the IMPATT diode is kept lower by 10°C compared with the IMPATT diode of the LO in panel UP. The junction temperature rise of the IMPATT diode in panel AP is 173°C, which offers an MTBF of 7.8×10^5 h.

[3] Waveguide inside dimensions in millimeters: R-260:8.636 × 4.318, R-320:7.122 × 3.556, R-500:4.775 × 2.388, R-740:3.099 × 1.549.

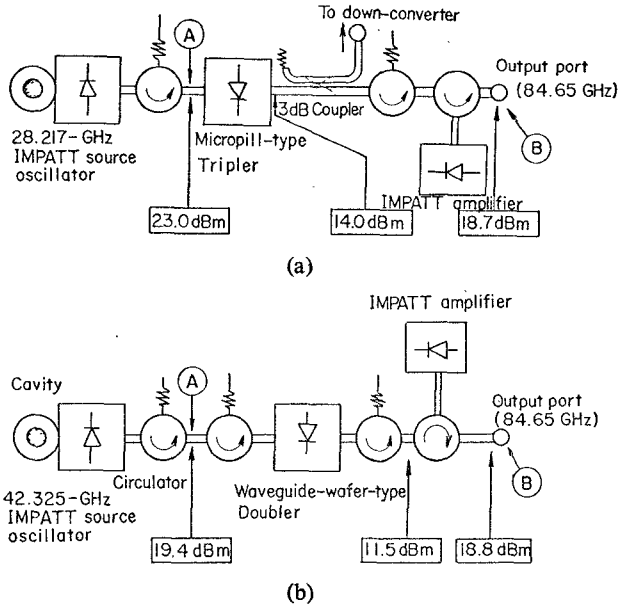

Fig. 7. LO constructions and power levels. (a) The LO in panel UP. (b) LO in panel AP.

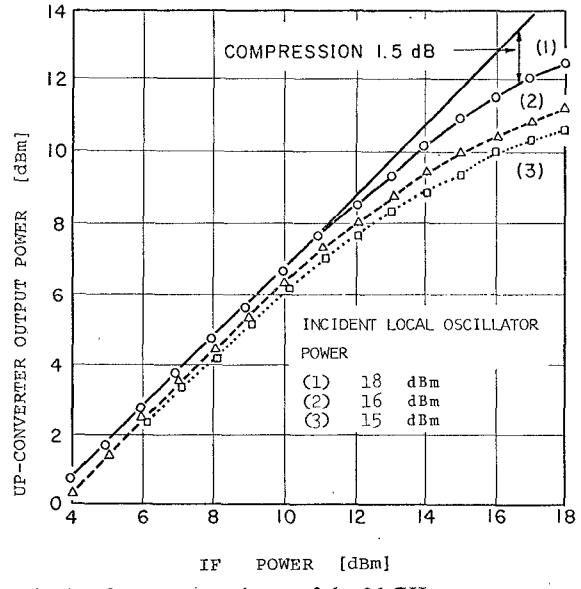

Fig. 8. Output versus input of the 86-GHz upconverter.

B. Upconverter

The diode is biased backward by the rectified current through a resistor connected in the dc circuit. Resistance is chosen so as to give the minimum conversion loss. The diode junction diameter is 7 μm. Electrical contact is made by a gold-plated whisker, the diameter of which is 30 μm.

Fig. 8 shows the input–output characteristics of the upconverter in panel UP. When the incident LO power and IF power are 18 and 16.7 dBm, respectively, 11.9 dBm of output power (which corresponds to a panel output power of 8.9 dBm) is obtained with a gain compression of 1.5 dB. The estimated junction temperature rise is 58.7°C. Accord-

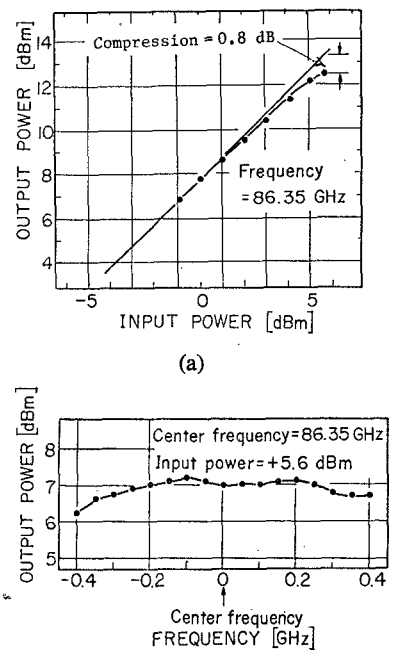

Fig. 9. (a) Output power versus input power. (b) Output power versus frequency.

ing to (1), this upconverter is expected to have a failure rate less than 100 fits when the ambient temperature is 25°C. The upconverter in panel AP yields 7.9 dBm with a compression of 0.7 dB, when the incident LO and IF powers are 16.3 and 12.6 dBm, respectively. The junction temperature rise is 33°C. At this junction temperature the expected failure rate is negligible.

C. IMPATT Power Amplifier

In this section the negative resistance amplifier for amplifying the upconverter output power used in panel AP is described. The amplifier is of a reflection type, and consists of a waveguide wafer-type diode holder, a circulator, and a movable waveguide short. The waveguide wafer consists of an IMPATT diode which is mounted on a diamond heat sink, and a coaxial cavity which is cross coupled to the waveguide [14], [18].

Fig. 9 shows characteristics of the 86-GHz amplifier. The junction diameter is 27 μm and the breakdown voltage is 11 V. Fig. 9(a) shows the power transfer characteristics. The output power is 12.6 dBm when the input is 5.6 dBm (gain compression = 0.8 dB). Fig. 9(b) shows the output power versus frequency characteristics for an input power of 5.6 dBm. The output deviation is less than 1 dB for the frequency range $f_0 \pm 400$ MHz ($f_0 = 86.35$ GHz). Fig. 10 shows the output pulse response for the case where the input phase abruptly changes from 0 to π rad. The output waveform distortion is very small. Measured group delay time was less than 0.5 ns in the frequency range $f_0 \pm 400$ MHz. The junction temperature rise of the diode is 170°C and MTBF is 9.8×10^5 h when the ambient temperature is 25°C.

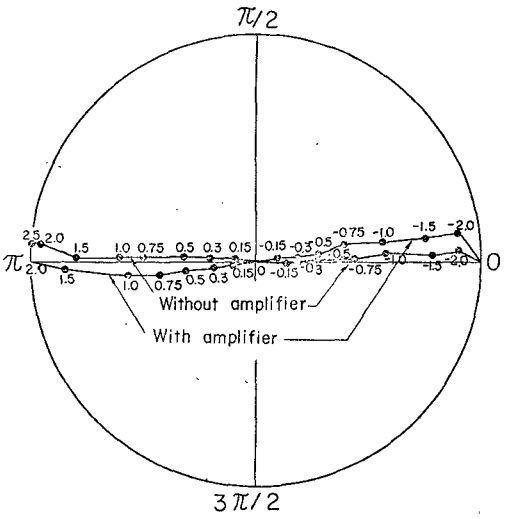

Fig. 10. Transient response of the IMPATT amplifier. Input is a $0 \sim \pi$ phase step. Numerical values in this figure express the transient time (nanoseconds).

TABLE VI
OVERALL CHARACTERISTICS OF 86-GHz TRANSMITTER–RECEIVER PANELS

			Panel UP	Panel AP
Carrier	f_0 = 86.35 GHz			
IF	1.7 GHz			
Transmitter	Panel output power [dBm]		8.4	10.7
	Up-converter	Output power [dBm]	10.4	7.9
		Compression [dB]	1.1	0.7
		Incident local power [dBm]	18	16.3
		Incident IF power [dB]	16.2	12.6
		Junction temperature [°C]	81	58
	IMPATT amplifier	Output power [dBm]		12.6
		Compression [dB]		0.8
		Gain [dB]		7.0
		Junction temperature [°C]		195
	Amplitude deviation [dB] $f_0 \pm 400$ MHz		1.1	1.0
Receiver	Down-converter	Conversion loss [dB]	5.8	7.6
		Incident local power [dBm]	6	7
		Junction temperature [°C]	< 40	<40
	Overall noise figure [dB]		11.4	13.5
Local oscillator	Frequency stability		$<\pm 7\times10^{-5}$	$<\pm 7\times10^{-5}$
	Construction		Fig.8(a)	Fig.8(b)
	Output power [dBm]		18.7	18.8
	Source Oscillator	Output power [dBm]	23	19.4
		Junction temperature [°C]	157	156
	Multiplier	Conversion loss [dB]	9.0	7.3
		Output power [dBm]	14.0	11.5
		Junction temperature [°C]	88	80
	IMPATT amplifier	Output power [dBm]	18.7	18.8
		Gain [dB]	6.7	7.3
		Junction temperature [°C]	205	198

Note: 1) The ambient temperature is assumed to be 25°C. 2) Junction diameter of the downconverter diode = 3 μm. 3) Total failure rate of above components = 2270 fits (panel UP), 2350 fits (panel AP).

D. Overall Characteristics of Transmitter–Receiver Panels

The overall characteristics of panels UP and AP are summarized in Table VI. The total failure rate is less than 2400 fits.

CONCLUSION

Reliability of semiconductor active devices is determined by the junction temperature of diodes used. The practical devices and equipment for a guided millimeter-wave transmission system should be highly reliable and produce

high powers. In this paper the reliability of LO's, upconverters, IMPATT amplifiers, and transmitter–receivers was calculated and the reliability allotment to each component was made for given reliabilities. The analysis shows that an optimum amplifier gain exists which gives the maximum transmitter power. It also shows that power increase by introducing an IMPATT amplifier following the upconverter is about 3 dB when the total MTBF is 10^5 h. Active components and transmitter–receiver modules have been constructed for use at 86 GHz based upon the reliability design as well as RF performance design.

Appendix
Power Gain, Output Power, and Compression of an IMPATT Amplifier

An IMPATT amplifier is composed of an IMPATT diode, a circulator, a signal source, and a load. Let us consider the case where the circuit is adjusted so as to give maximum power gain. Then the equivalent circuit seen from the diode terminal is expressed as a parallel connection of three components: $-G$ (diode negative conductance); G_L (load conductance); and I (current source).

The available power of the signal source P_{in}, power gain G_A, and output power P_{amp} are expressed as

$$P_{in} = I^2/4G_L$$
$$G_A = (G_L + G)^2/(G_L - G)^2$$
$$P_{amp} = P_{in} \cdot G_A. \tag{A1}$$

Negative conductance of an IMPATT diode is a function of the RF voltage across the diode V_D, and is approximately expressed as [12]–[14]

$$G = G_M(V_M - V_D)^2/V_M{}^2 \tag{A2}$$

where G_M is the maximum absolute value of the negative conductance, and V_M is the RF voltage across the diode when the negative conductance becomes zero. V_D is expressed by the current source and conductances as

$$V_D = I/(G_L - G). \tag{A3}$$

The maximum oscillation power P_{osc} of the preceding diode is obtained when $G = G_M/2$, and is given by

$$P_{osc} = G_M V_M{}^2/4. \tag{A4}$$

From (A1)–(A4), one can obtain the ratio of the amplifier output power to the maximum oscillation power μ ($\mu = P_{amp}/P_{osc}$), the gain compression ξ ($\xi = G_{max}/G_A$; G_{max} is the power gain when $G = G_M$), and G_A as follows:

$$\mu = (g_L + g)^2(1 - g)/g_L$$
$$G_A = (g_L + g)^2/(g_L - g)^2$$
$$\xi = [(g_L - g)^2/(g_L + g)^2] \cdot [(g_L + 1)^2/(g_L - 1)^2] \tag{A5}$$

where $g_L = G_L/G_M$ and $g = G/G_M$.

By eliminating g_L and g from the preceding equations, one can obtain the relation among μ, G_A, and ξ as

$$\mu = \frac{\sqrt{\xi G_A} + 1}{\sqrt{\xi G_A} - 1} \cdot \frac{4G_A}{(1 + \sqrt{G_A})^2} \cdot \left(1 + \frac{\sqrt{\xi G_A} + 1}{\sqrt{\xi G_A} - 1} \cdot \frac{1 - \sqrt{G_A}}{1 + \sqrt{G_A}}\right). \tag{A6}$$

Acknowledgment

The authors wish to thank Dr. K. Miyauchi, Dr. S. Shimada, and Dr. Y. Sato for their helpful guidance and fruitful discussions. The authors also wish to express their thanks to the members of Nippon Electric Company, Ltd., and to the members of Fujitsu Laboratories, Ltd., for their cooperation in manufacturing.

References

[1] Technical papers of Conference on Trunk Telecommunications by Guided Waves, Sept. 29/Oct. 2, 1970, London.
[2] T. E. Abele, D. A. Alsberg, and P. T. Huchison, "A high-capacity digital communication system using TE_{01} transmission in circular waveguide," *IEEE Trans. Microwave Theory Tech.*, vol. MTT-23, pp. 326–333, April 1975.
[3] R. W. White, M. B. Read, and A. J. Moore, "Recent British work on millimetric waveguide system," *IEEE Trans. Communication Soc.*, vol. COM-22, pp. 1378–1390, Sept. 1974.
[4] J. R. Mahieu, J. N. Marchalot, J. P. Boujet, G. L. Coz, P. Gibeau, and J. V. Bouvet, "Technologies avancées dévelopées par l'industrie pour les études sur le guide d'ondes circulaire," *Annales Télécommunications*, vol. 29, pp. 443–464, Sept./Oct. 1974.
[5] G. Hanke, T. Adachi, and D. Briggmann, "640 Mbit/s PCM regenerator for a broadband experimental waveguide system," in *Proc. 1974 European Microwave Conf.*, pp. 634–638.
[6] P. Bernardi, G. C. Corazza, G. Faliciasecca, R. Koch, G. Magni, G. A. Mastellari, G. B. Stracca, and F. Vardoni, "Italian experimental equipment for high bit rate transmission on circular waveguide," in *Proc. 1974 European Microwave Conf.*, pp. 619–623.
[7] K. Miyauchi, S. Seki, N. Ishida, and K. Izumi, "W-40G guided millimeter-wave transmission system," *Review of Electrical Communication Laboratories*, vol. 23, pp. 707–741, July/August 1975.
[8] H. J. Kuno and P. H. Pusateri, "Use of solid-state components for mm-wave measurements," *Microwave Journal*, vol. 17, no. 8, pp. 35–40, August 1974.
[9] Y. Sato and M. Fujimoto, "Millimeter-wave GaAs diodes," *Review of Electrical Communication Laboratories*, vol. 23, pp. 939–947, July/August 1975.
[10] K. Suzuki, "Millimeter-wave Si IMPATT diodes," *Review of Electrical Communication Laboratories*, vol. 23, pp. 948–958, July/August 1975.
[11] M. Ohmori, "Optimum junction diameters of 80-GHz band IMPATT diodes," *Proc. IEEE*, vol. 62, pp. 537–538, April 1974.
[12] M. S. Gupta, "Large-signal equivalent circuit for IMPATT-diode characterization and its application to amplifiers," *IEEE Trans. Microwave Theory Tech.*, vol. MTT-21, pp. 689–694, Nov. 1973.
[13] H. J. Kuno, "Analysis of nonlinear characteristics and transient response of IMPATT amplifiers," *IEEE Trans. Microwave Theory Tech.* vol. MTT-21, pp. 694–702, Nov. 1973.
[14] H. J. Kuno and D. L. English, "Nonlinear and large signal characteristics of millimeter-wave IMPATT amplifiers," *IEEE Trans. Microwave Theory Tech.*, vol. MTT-21, pp. 703–706, Nov. 1973.
[15] M. Akaike, N. Kanmuri, and H. Kato, "Junction-temperature-rise calculation of millimeter-wave diodes," in 1974 IECE (Japan) National Convention, paper 964.
[16] H. C. Torrey and C. A. Whitmer, *Crystal Rectifiers*. New York: McGraw-Hill, 1948.
[17] H. Kato and K. Kaneko, "Junction temperature elevation of varactor diodes," *Trans. IECE* (Japan), vol. 58-B, pp. 385–392, August 1975.
[18] H. Hayashi, F. Iwai, T. Fujita, M. Akaike, and H. Kato, "80 GHz IMPATT amplifier," in 1974 IEEE International Solid-State Circuit Conf., paper THAM9.6.